Footprints of electron correlation in strong-field double ionization of Kr close to the sequential-ionization regime

Xiaokai Li,[1] Chuncheng Wang,[1,*] Zongqiang Yuan,[2] Difa Ye,[3] Pan Ma,[1] Wenhui Hu,[1] Sizuo Luo,[1] Libin Fu,[3,4,†] and Dajun Ding[1,‡]

[1]*Institute of Atomic and Molecular Physics, Jilin University, Changchun 130012, People's Republic of China*

[2]*Science and Technology on Plasma Physics Laboratory, Research Center of Laser Fusion, China Academy of Engineering Physics, Mianyang 621900, People's Republic of China*

[3]*Laboratory of Computational Physics, Institute of Applied Physics and Computational Mathematics, Beijing 100088, People's Republic of China*

[4]*Graduate School, China Academy of Engineering Physics, Beijing 100193, People's Republic of China*

(Received 10 February 2017; published 25 September 2017)

By combining kinematically complete measurements and a semiclassical Monte Carlo simulation we study the correlated-electron dynamics in the strong-field double ionization of Kr. Interestingly, we find that, as we step into the sequential-ionization regime, there are still signatures of correlation in the two-electron joint momentum spectrum and, more intriguingly, the scaling law of the high-energy tail is completely different from early predictions on the low-Z atom (He). These experimental observations are well reproduced by our generalized semiclassical model adapting a Green-Sellin-Zachor potential. It is revealed that the competition between the screening effect of inner-shell electrons and the Coulomb focusing of nuclei leads to a non-inverse-square central force, which twists the returned electron trajectory at the vicinity of the parent core and thus significantly increases the probability of hard recollisions between two electrons. Our results might have promising applications ranging from accurately retrieving atomic structures to simulating celestial phenomena in the laboratory.

DOI: 10.1103/PhysRevA.96.033416

I. INTRODUCTION

Strong-field double ionization (SFDI) of atoms is typically divided into two categories: sequential and nonsequential [1]. In sequential double ionization (SDI), the two electrons are removed one by one, and thus a single-active-electron (SAE) treatment is believed to be valid for both electrons. Nonsequential double ionization (NSDI), in contrast, proceeds by recollision of an initially released electron driven back by the oscillating laser field, hitting head on the parent ion and dislodging another bound electron [2]. Even though this general scenario is well established, a comprehensive understanding of the microscopic dynamics is far from complete. There, a significant target dependence of SFDI does exist and the underlying mechanisms are much richer than expected. Specifically, with the in-depth study of SFDI, new mechanisms such as postrecollision backscattering [3–7], multiple recollision [8,9], recollision-induced excitation tunneling [10], and sequential release from double excitation [11] were proposed, and in some cases, the quantum interference of different pathways was invoked to explain the data observed [12–15], which certainly go far beyond the early proposed field-assisted $(e,2e)$ process. More recently, surprisingly, it was found in experiments that the behavior of SFDI of high-Z atoms (the earliest studied rare-gas atom, Xe) was remarkably different from low-Z rare-gas atoms, i.e., He, Ne, and Ar, and inner-shell electron screening effects for high-Z atoms are believed to play important roles [16]. However, how the screening effect in SFDI evolves from the low-Z to high-Z atoms has yet to be discussed, and a fully differential measurement on SFDI of Kr is missing.

Moving to the SDI regime at higher laser intensities, there exists another ongoing debate focusing on the question of whether the electron correlation is or is not totally smeared out. Historically, the SDI regime was anticipated to be physically clean, without much discernible controversy between experimental observations and theoretical predictions on the ion yield [17] or even the electron correlation [18]. This situation, however, is challenged by recent experiments. In Ref. [19], a strong angular correlation between two electrons was detected in the intensity regime that was usually attributed to the SDI regime, suggesting that the expected successive ionization steps are indeed not independent. More recently, Pfeifer and co-workers measured the released time of SDI with an attoclock technique and found that the ionization of the second electron occurred significantly earlier than predicted [20]. There, controversy seems to still exist because further refined theories either including [21] or excluding [22] the electron-electron correlation can well reproduce the experimental data. Thus, a consensus on whether an electron correlation is essential in SDI is still lacking.

In this article, we report a fully differential measurement on SFDI of krypton in near-infrared laser fields. By choosing the Kr atom, we are able to bridge the gap between low-Z (e.g., He) and high-Z (e.g., Xe) atoms and reveal the target dependence of the screening effect. Furthermore, our differential measurements cover a wide range of laser intensities crossing from the NSDI plateau to the SDI domain, and thus offer the opportunity to answer how electron correlation evolves from the NSDI to SDI regime. In the NSDI regime, the measurements on Kr show clear crossover behavior in comparison with early results on Ar and Xe. By increasing the laser intensity well into the SDI regime, which is traditionally expected to be well

*ccwang@jlu.edu.cn
†lbfu@iapcm.ac.cn
‡dajund@jlu.edu.cn

described by a single-active-electron (SAE) approximation, however, we find that the electron correlation still gets involved in a subtle way. A two-electron joint momentum spectrum reveals clear signatures of electron correlation and, moreover, the sum-energy spectrum shows long tails extending far beyond the prediction of SDI models. Upon closer inspection, we further find that the scaling law of the high-energy tail is completely different from an early prediction on He by *ab initio* simulations [23], pointing to multielectron effects beyond the capability of the heliumlike model. However, currently solving the fully dimensional time-dependent Schrödinger equation for double ionization of an atom with more than two electrons is computationally cumbersome. Moreover, the potential development of a time-dependent density functional theory (TDDFT) for this kind of experiment is not very likely to happen because current well-established TDDFT approaches do not even describe double excitations (see, e.g., Refs. [24,25]). Thus, it is highly desirable to develop and refine classical or semiclassical models. As will be shown later, by suitably taking into account the shielding effect of the inner-shell electrons [26], we are able to qualitatively reproduce the experimental observations and further disentangle the underlying physical mechanisms by tracing back the classical trajectories.

II. EXPERIMENTAL METHODS

We performed the measurements in cold-target recoil-ion-momentum spectroscopy (COLTRIMS) with linearly polarized femtosecond (fs) laser pulses (50 fs, 800 nm, 1 kHz) which were focused by a concave mirror ($f = 7.5$ cm) onto a supersonic gas jet (seeded by He) [27]. The produced ions and electrons were guided towards two position-sensitive detectors by applying weak homogenous electric (3.7 V/cm) and magnetic (6.5 G) fields along the laser polarization axis. The electron rate in all experiments was controlled to below 0.2 per pulse to keep the false coincidence rate sufficiently low. We obtained correlated-electron momentum distributions by collecting the coincidence events of Kr^{2+} and one electron to avoid a detection dead time of electron-electron coincidence measurements, and the longitudinal momentum of the other electron was calculated according to momentum conservation [18]. For the electron sum-energy spectrum, both the longitudinal momentum and lateral momentum need to be included, with the latter having a poorer resolution, so we thus resort to a triple-coincidence measurement (two electrons and the doubly charged parent ion) to obtain a more reliable energy distribution. The peak laser intensity is calibrated by measuring the yield of Xe^{2+}/Xe^{+} with respect to intensity [28,29] and also the longitudinal momentum distribution of Ar^{2+} [30], and the agreement for these two methods is quite good.

III. RESULTS AND DISCUSSION

The measured ratio curve of Kr^{2+}/Kr^{+} as a function of laser intensity is shown in Fig. 1(a), where a typical knee structure is clearly visualized, indicating that we have covered a wide range of laser intensities from NSDI to SDI. Four typical laser intensities are then chosen for further analysis. The associated longitudinal momentum distributions of Kr^{2+} are shown in Fig. 1(b). As the laser intensity increases, the

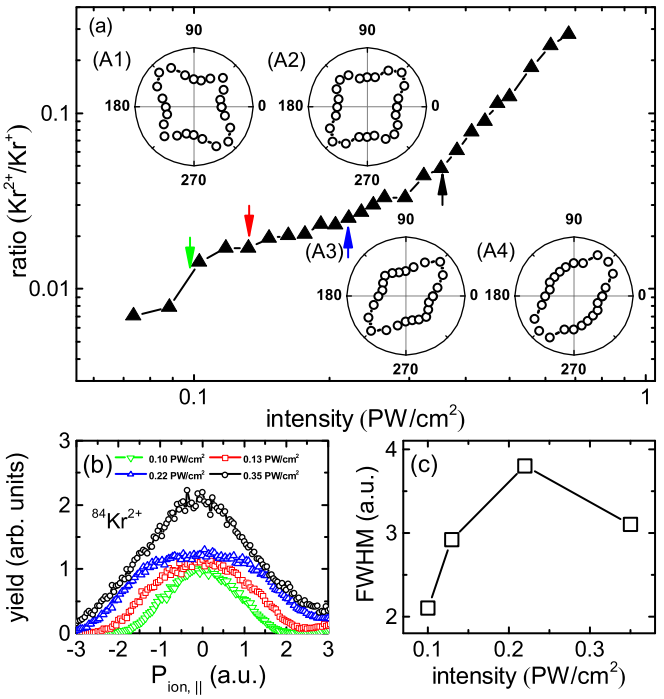

FIG. 1. (a) The measured ratio of double-over-single ionization yield as a function of the laser intensity. (b) The longitudinal momentum distributions of Kr^{2+} at four typical laser intensities, as indicated by the arrows labeled in (a). The widths (FWHM) of the ion momentum spectra are shown in (c) and the angular distributions of correlated-electron momentum maps at the corresponding intensities are illustrated in (A1)–(A4).

momentum spectra develop from a Gaussian distribution to a broad single hump structure and then again a Gaussian distribution. Quantitatively, the full width at half maximum (FWHM) of the momentum distribution first increases as the laser intensity increases, and then rapidly decreases around an intensity of 3.5×10^{14} W/cm^2 [Fig. 1(c)]. This can be explained as a result of the changes in the line shape from a broad hump to a Gaussian, which signifies the appearance of SDI. We note that our measurements complete the picture of atomic-species dependence of the ion momentum, in the sense that under similar Keldysh parameters one observes a continuous development from a double-hump structure in He and Ne through a plateau structure in Ar [31], to a broad single-hump structure in Kr (this article), and finally arriving at a Gaussian distribution in Xe [16]. In this sense, Kr is an indispensable candidate for studying the transition behavior from low-Z to high-Z atoms.

To reveal the straightforward picture behind the electron dynamics of NSDI of Kr, we measure the correlated-electron momentum spectra [shown in Figs. 2(i)–(l)] and then convert them into polar plots with the polar angle defined as $\theta = \arg[p_{\|}(e_1) + ip_{\|}(e_2)]$, where $\theta \in [0,2\pi)$. The angular distributions are shown in Figs. 1(A1)–1(A4), which exhibit rich structures and strongly depend on the laser intensity, evolving from an inhomogeneous distribution with higher populations in the second and fourth quadrants [Figs. 1(A1) and 2(i)] to an elongated pattern with substantially more population in the first and third quadrants [Figs. 1(A3) and 2(k)]. This is a

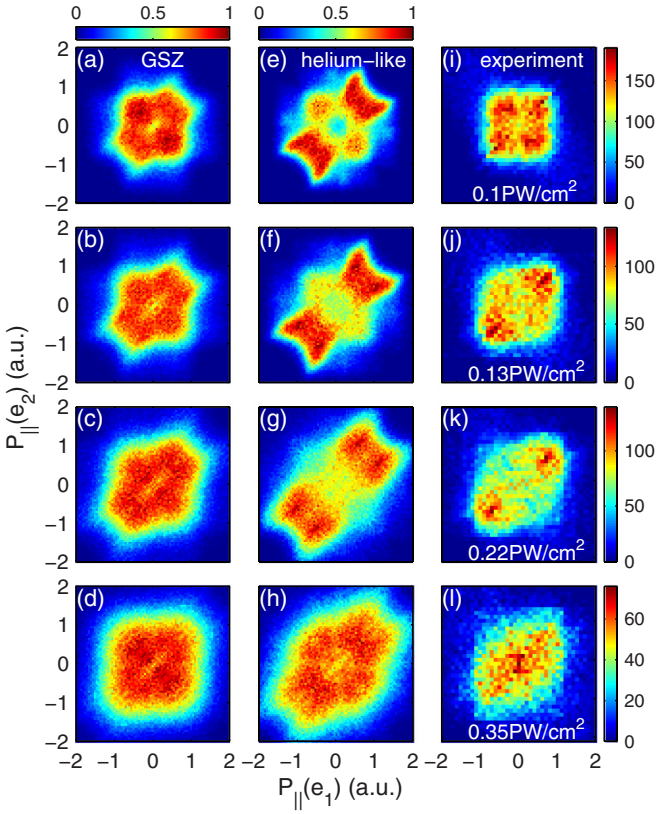

FIG. 2. The measured [(i)–(l)] and calculated two-electron joint momentum spectrum with the GSZ model [(a)–(d)] and the heliumlike model [(e)–(h)]. The laser intensities are indicated in the last column and each row has the same intensity. In the theoretical calculations, all doubly ionized trajectories are allowed to evolve freely for 1000 more cycles after turning off the laser field to ensure the convergence of the near-zero momenta.

typical signature of recollision and NSDI, universal for He, Ne, and Ar, and thus is not surprising. However, as we step forward to 3.5×10^{14} W/cm^2, which is expected to be in the SDI regime according to the measurements on ion yield and ion momentum [recall Figs. 1(a) and 1(b)], there still exists a weak dominance of side-by-side emission [Figs. 1(A4) and 2(l)]. This clearly reveals the electron correlation in the SDI regime, which is smeared out in the measurements of ion yield and ion momentum.

In order to clarify the mechanism behind the observed laser-intensity-dependent electron correlation in SFDI of Kr, we have performed numerical simulations with two semiclassical models, i.e., the widely used heliumlike model and an improved Green-Sellin-Zachor (GSZ) model. In both models, one electron is released at the outer edge of the field-suppressed Coulomb barrier along the field direction through quantum tunneling with a rate given by the Ammosov-Delone-Krainov (ADK) theory. The tunneled electron has a Gaussian distribution on the transverse velocity and zero longitudinal velocity. The bound electron is sampled from a microcanonical distribution. The subsequent evolution of the two electrons with the above initial conditions is governed by Newton's equations of motion. A recollision-induced excitation-tunneling effect of both electrons has been included by allowing the electrons to tunnel through the potential barrier whenever they reach the outer turning point, with the tunneling probability given by the Wentzel-Kramers-Brillouin (WKB) approximation. For high-Z atoms, to take into account the influence of the inner-shell electrons, the heliumlike model is improved by adopting the GSZ potential for the interaction between the core (Z protons plus $Z-2$ nonactive electrons) and two active electrons. More details of the model can be found in Ref. [26] and references therein.

We emphasize that the initial time (tunneling instant) in our simulation is randomly distributed over the whole pulse duration and is weighted by the ADK rate $w_{\rm ADK}(t_0)$ times a depletion factor $\chi(t_0)=e^{-\int_{-\infty}^{t_0} w_{\rm ADK}(t')dt'}$. Here, the laser pulse has a $\sin^2$ envelope with a total of 20 optical cycles. The volume effect is also taken into account by assuming a laser beam with a Gaussian radial distribution. The above two concerns are indispensable when the laser intensity is increased close to the saturation regime. The proceeding semiclassical model has provided deep insight into the dynamics of correlated electrons in SFDI, both for the low-Z and high-Z rare-gas atoms, but with a different physical picture. For low-Z atoms, it was shown that the heliumlike model was accurate enough to reproduce most of the features observed in SFDI of He and Ar, including the fingerlike structure [3,4] and the transition from correlation to anticorrelation in the below-threshold regime [8]. The Coulomb focusing [32] (or Coulomb singularity [33]) of the nuclear potential was identified to play a key role [7,34]. However, for high-Z atoms (e.g., Xe), the dynamical screening effect of the inner-shell electrons become dominant and thus the GSZ model works much better than the heliumlike model [16,26]. As an atom lying in between Ar and Xe, one thus expects that Kr will show an even more complicated electron correlation dynamics due to the competition between Coulomb focusing of the nuclei and the dynamical screening of the inner-shell electrons. This is evidenced by the two-electron joint momentum spectrum shown in Figs. 2(a)–2(h), calculated by two models for comparison.

In general, the GSZ model calculations agree better with the experiments at lower intensities [Figs. 2(a) and 2(b)] where the momentum spectrum has a roughly round shape without a significant V-shaped (or fingerlike) structure in the first and third quadrants, while the heliumlike model calculations agree better with the experiments at higher intensities [Figs. 2(g) and 2(h)] where the momentum spectrum is substantially elongated and undergoes a transition from correlation back to anticorrelation (two bright spots appear again in the second and fourth quadrants) as the laser intensity enters the SDI regime. Thus, a single model (neither the heliumlike model nor the GSZ model) cannot solely reproduce all the experimental observations. This fact indicates the complex role of inner-shell electrons in NSDI of Kr in comparison with Ar and Xe. Specifically, the dynamical screening effect of inner-shell electrons is found to be more important at lower laser intensities, which can be understood as a result of the tunneled electron in this case having a shorter quiver length, and thus is typically trapped closer to the atomic core, leading to the atomic structure playing a more important role.

More strong evidence for the existence of electron correlation in the SDI regime is revealed by the sum-energy

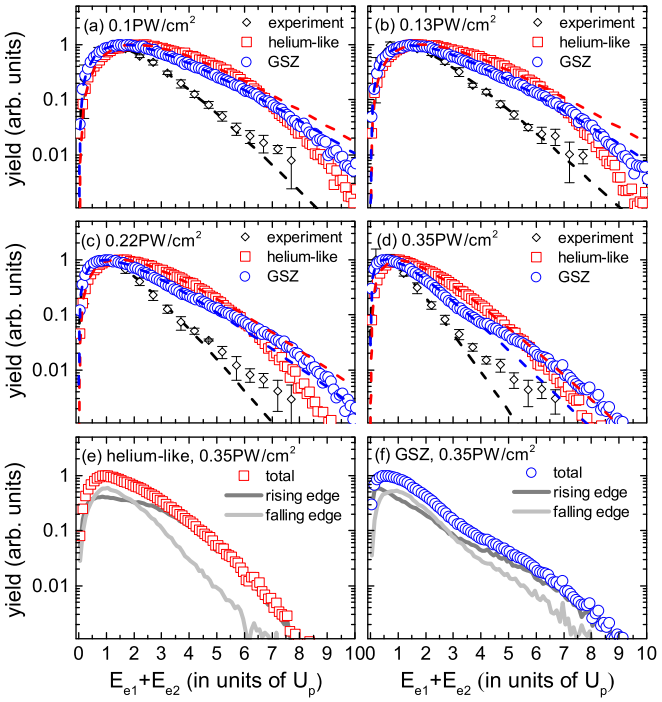

FIG. 3. (a)–(d) The two-electron sum-energy spectra measured and calculated with the heliumlike model and the GSZ model, respectively, along with fittings by a gamma-distribution function at different laser intensities. In (e) and (f), the sum-energy spectra at 0.35 PW/cm^2 are divided into two parts contributed by those tunneled electrons released at the rising edge (dark gray) and the falling edge (light gray) of the laser field.

spectra of two electrons, as shown in Figs. 3(a)–3(d) along with fittings on the data by the gamma-distribution function $f(E) = cE^{\alpha}e^{-\beta E}$. This kind of study about the sum-energy spectra has at least two advantages [35]: First, the sum energy contains all of the information about the DI system, including both the longitudinal (field-dominant) and the lateral (field-free) momenta of both electrons, and, moreover, it is plotted in a logarithmic scale, which might reveal further details that are hidden in the correlated-electron momentum spectrum. As can be seen in Fig. 3, the data show a good match with the fittings over the entire energy range when the laser intensity is in the NSDI plateau regime [Figs. 3(a) and 3(b)]. By increasing the laser intensity to the SDI region [diamonds in Fig. 3(d)], however, one finds long tails that significantly deviate from the fittings beyond $4U_p$, and, more interestingly, the long tails bend upward rather than downward, in contrast to the predictions on He [23]. This is rather surprising at 3.5×10^{14} W/cm^2, for which, according to the estimation of SDI theory, $4U_p$ is the cutoff position and the spectrum is expected to drop sharply.

The superiority of the generalized GSZ model to reveal the scaling law of the high-energy tail in the sum-energy spectrum is very evident, as shown in Figs. 3(a)–3(d), where the sum-energy spectra are calculated by the heliumlike model and the GSZ model, respectively, for a direct panel-to-panel comparison with the experimental data. It can be seen that only the GSZ model, by suitably taking into account the inner-shell electron screening effect, can well reproduce

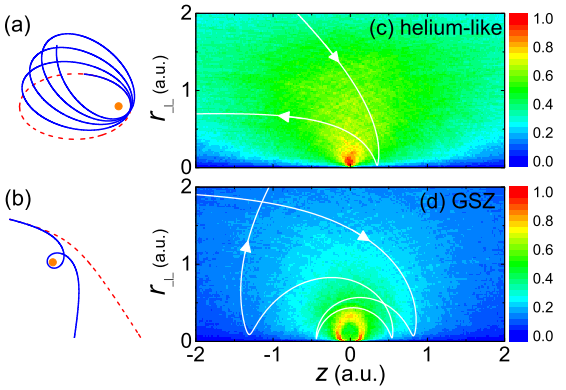

FIG. 4. Typical trajectories of (a) a bound electron and (b) a free electron under the influence of an inverse-square (red dashed line) or non-inverse-square (blue solid line) central force. (c) and (d) show the trajectory density of the returned electrons in the vicinity of the parent ion. In general, the GSZ potential has a stronger focusing effect via twisting the trajectories around the core, as demonstrated by the sampled orbits (white curves).

the upward-bending long tails of the sum-energy spectra [circles in Fig. 3(d)], while the heliumlike model predicts a sharply downward-bending high-energy tail [see, e.g., squares in Fig. 3(a)], similar to early predictions on He [23] but contradicting the present measurements on Kr. The upward-bending long tail indicates the large cross section of high-energy double ionization and thus a high probability of hard recollisions.

To further reveal the physical mechanism of hard recollisions, we separate the sum-energy spectra into two parts contributed by tunneled electrons released at the rising edge and the falling edge of the laser field, respectively [dark gray and light gray curves in Figs. 3(e) and 3(f)]. Clearly, most of the high-energy double ionizations are produced by those tunneled electrons released during the rising edge of the laser field. This is quite surprising because these electrons have longer trajectories and larger divergent angles. Thus, without strong Coulomb focusing [32] of the GSZ core, they are not able to efficiently return to the parent ions. Furthermore, for a fixed laser intensity, the spectrum calculated by the GSZ model generally extends to a higher sum-energy in comparison with that of the heliumlike model, which can be understood as a result of the fact that the GSZ core has a stronger Coulomb singularity [33], because the effective nuclear charge increases from 2 to Z as the radial position goes from infinity to zero.

The stronger focusing effect of the GSZ potential is clearly revealed in Figs. 4(c) and 4(d), where we launch a statistics on the trajectory density over 10^4 randomly sampled orbits of the tunneled-and-driven-back electrons in the vicinity of the parent core. The higher electron density surrounding the GSZ core can be understood as a result of the twist of the electron trajectories due to the non-inverse-square central force. This significantly enhances the probability of hard recollisions between the returned and the bound electrons, finally disclosing the physical origin of the upward-bending high-energy tail.

IV. CONCLUSION

In conclusion, we have comprehensively studied the correlated-electron dynamics of the strong-field double ionization of Kr with kinematically complete measurements. We first measured the ion yield and the ion momentum as a function of the laser intensity and confirmed that we have penetrated into the SDI regime, where, however, the two-electron joint momentum spectrum still reveals a visible correlated pattern and the two-electron sum-energy spectrum also shows long tails far exceeding the estimation of SAE models as well as *ab initio* calculations on He. By combining semiclassical simulations with a generalized GSZ model, we reveal the pivotal role of Coulomb focusing and Coulomb singularity of nuclei competing with the screening effect of the inner-shell electrons. These findings are of broad interest and probably might have some cross-impact in the future. First, the sensitive dependence of the sum-energy spectrum on the atomic core potential offers a promising opportunity to accurately retrieve the inner-shell atomic structure as pioneered, for example, by Refs. [36,37]. Second, the physical mechanism is closely related to the well-known apsidal precession of planetary motion [38], thus offering the possibility to simulate celestial phenomena in the laboratory.

ACKNOWLEDGMENTS

This work was supported by the National Basic Research Program of China under Grant No. 2013CB922200, by the NNSFC under Grants No. 11774130, No. 11304117, No. 11534004, No. 11127403, No. 11374040, No. 11604312, No. 11674034, and No. 11374122, by the Foundation of President of CAEP (Grant No. 2014-1-029), and by the China Postdoctoral Science Foundation under Grants No. 2013M530137 and No. 2015T80293.

[1] W. Becker, X. Liu, P. J. Ho, and J. H. Eberly, Rev. Mod. Phys. **84**, 1011 (2012).
[2] P. B. Corkum, Phys. Rev. Lett. **71**, 1994 (1993).
[3] A. Rudenko, V. L. B. de Jesus, T. Ergler, K. Zrost, B. Feuerstein, C. D. Schroter, R. Moshammer, and J. Ullrich, Phys. Rev. Lett. **99**, 263003 (2007).
[4] A. Staudte, C. Ruiz, M. Schoffler, S. Schossler, D. Zeidler, T. Weber, M. Meckel, D. M. Villeneuve, P. B. Corkum, A. Becker, and R. Dorner, Phys. Rev. Lett. **99**, 263002 (2007).
[5] S. L. Haan, J. S. Van Dyke, and Z. S. Smith, Phys. Rev. Lett. **101**, 113001 (2008).
[6] A. Emmanouilidou, Phys. Rev. A **78**, 023411 (2008).
[7] D. F. Ye, X. Liu, and J. Liu, Phys. Rev. Lett. **101**, 233003 (2008).
[8] Y. Liu, S. Tschuch, A. Rudenko, M. Durr, M. Siegel, U. Morgner, R. Moshammer, and J. Ullrich, Phys. Rev. Lett. **101**, 053001 (2008).
[9] S. L. Haan, Z. S. Smith, K. N. Shomsky, and P. W. Plantinga, J. Phys. B **41**, 211002 (2008).
[10] B. Feuerstein, R. Moshammer, D. Fischer, A. Dorn, C. D. Schroter, J. Deipenwisch, J. R. Crespo Lopez-Urrutia, C. Hohr, P. Neumayer, J. Ullrich, H. Rottke, C. Trump, M. Wittmann, G. Korn, and W. Sandner, Phys. Rev. Lett. **87**, 043003 (2001).
[11] N. Camus, B. Fischer, M. Kremer, V. Sharma, A. Rudenko, B. Bergues, M. Kubel, N. G. Johnson, M. F. Kling, T. Pfeifer, J. Ullrich, and R. Moshammer, Phys. Rev. Lett. **108**, 073003 (2012).
[12] D. I. Bondar, W. K. Liu, and M. Y. Ivanov, Phys. Rev. A **79**, 023417 (2009).
[13] Z. Chen, Y. Liang, and C. D. Lin, Phys. Rev. Lett. **104**, 253201 (2010).
[14] X. L. Hao, J. Chen, W. D. Li, B. Wang, X. Wang, and W. Becker, Phys. Rev. Lett. **112**, 073002 (2014).
[15] A. S. Maxwell and C. F. Faria, Phys. Rev. Lett. **116**, 143001 (2016).
[16] X. Sun, M. Li, D. Ye, G. Xin, L. Fu, X. Xie, Y. Deng, C. Wu, J. Liu, Q. Gong, and Y. Liu, Phys. Rev. Lett. **113**, 103001 (2014).
[17] U. Eichmann, M. Dorr, M. Maeda, W. Becker, and W. Sandner, Phys. Rev. Lett. **84**, 3550 (2000).
[18] T. Weber, H. Giessen, M. Weckenbrock, G. Urbasch, A. Staudte, L. Spielberger, O. Jagutzki, V. V. Mergel, M. Vollmer, and R. Dörner, Nature (London) **405**, 658 (2000).
[19] A. Fleischer, H. J. Worner, L. Arissian, L. R. Liu, M. Meckel, A. Rippert, R. Dorner, D. M. Villeneuve, P. B. Corkum, and A. Staudte, Phys. Rev. Lett. **107**, 113003 (2011).
[20] A. N. Pfeiffer, C. Cirelli, M. Smolarski, R. Dörner, and U. Keller, Nat. Phys. **7**, 428 (2011).
[21] Y. Zhou, C. Huang, Q. Liao, and P. Lu, Phys. Rev. Lett. **109**, 053004 (2012).
[22] X. Wang and J. H. Eberly, J. Chem. Phys. **137**, 22A542 (2012).
[23] A. Emmanouilidou, J. S. Parker, L. R. Moore, and K. T. Taylor, New J. Phys. **13**, 043001 (2011).
[24] M. Lein and S. Kümmel, Phys. Rev. Lett. **94**, 143003 (2005).
[25] M. Ruggenthaler and D. Bauer, Phys. Rev. Lett. **102**, 233001 (2009).
[26] Z. Yuan, D. Ye, J. Liu, and L. Fu, Phys. Rev. A **93**, 063409 (2016).
[27] J. Ullrich, R. Moshammer, A. Dorn, R. Dörner, L. Ph. H. Schmidt, and H. Schmidt-Böcking, Rep. Prog. Phys. **66**, 1463 (2003).
[28] J. L. Chaloupka, J. Rudati, R. Lafon, P. Agostini, K. C. Kulander, and L. F. DiMauro, Phys. Rev. Lett. **90**, 033002 (2003).
[29] C. Wang, D. Ding, M. Okunishi, Z.-G. Wang, X.-J. Liu, G. Prümper, and K. Ueda, Chem. Phys. Lett. **496**, 32 (2010).
[30] B. Feuerstein, R. Moshammer, and J. Ullrich, J. Phys. B **33**, L823 (2000).
[31] V. L. B. de Jesus, B. Feuerstein, K. Zrost, D. Fischer, A. Rudenko, F. Afaneh, C. D. Schörter, R. Moshammer, and J. Ullrich, J. Phys. B **37**, L161 (2004).
[32] D. Comtois, D. Zeidler, H. Pépin, J. C. Kieffer, D. M. Villeneuve, and P. B. Corkum, J. Phys. B **38**, 1923 (2005).
[33] A. Rudenko, K. Zrost, Th. Ergler, A. B. Voitkiv, B. Najjari, V. L. B. de Jesus, B. Feuerstein, C. D. Schröter, R. Moshammer, and J. Ullrich, J. Phys. B **38**, L191 (2005).
[34] D. F. Ye and J. Liu, Phys. Rev. A **81**, 043402 (2010).
[35] D. Ye, M. Li, L. Fu, J. Liu, Q. Gong, Y. Liu, and J. Ullrich, Phys. Rev. Lett. **115**, 123001 (2015).

[36] S. Micheau, Z. Chen, A. T. Le, J. Rauschenberger, M. F. Kling, and C. D. Lin, Phys. Rev. Lett. **102**, 073001 (2009).

[37] B. Wolter, M. G. Pullen, A.-T. Le, M. Baudisch, K. Doblhoff-Dier, A. Senftleben, M. Hemmer, C. D. Schröter, J. Ullrich, T. Pfeifer, R. Moshammer, S. Gräfe, O. Vendrell, C. D. Lin, and J. Biegert, Science **354**, 308 (2016).

[38] L. D. Landau and E. M. Lifshitz, *Mechanics* (Pergamon Press, New York, 1976).